

Rheology of Cubic Particles Suspended in a Newtonian Fluid

Colin D. Cwalina, Kelsey J. Harrison, and Norman J. Wagner

*Department of Chemical and Biomolecular Engineering
Center for Molecular Engineering and Thermodynamics
University of Delaware
Newark, DE 19716*

Supplemental Information

Validation of the Normal Force Inertia Correction

Inertia is known to create a negative contribution to the measured axial thrust at high shear rates. The correction of Turian⁴⁷ was used to account for the effect of inertia on the measured axial thrust:

$$(F_Z)_{\text{inertia}} = -0.075\pi\rho\Omega^2R^4 \quad (\text{S.1})$$

where $(F_Z)_{\text{inertia}}$ is the contribution to the axial thrust from inertia, ρ is the fluid density, Ω is the angular velocity, and R is the tool radius. In Figure S.1, experimental axial thrust data from a 40 mm 2° cone and plate tooling is reported for the Newtonian PEG-200 solvent over the range of shear rates probed in this study. Equation S.1 is also overlaid, thus validating it as an appropriate correction for the contribution of inertia to the measured axial thrust.

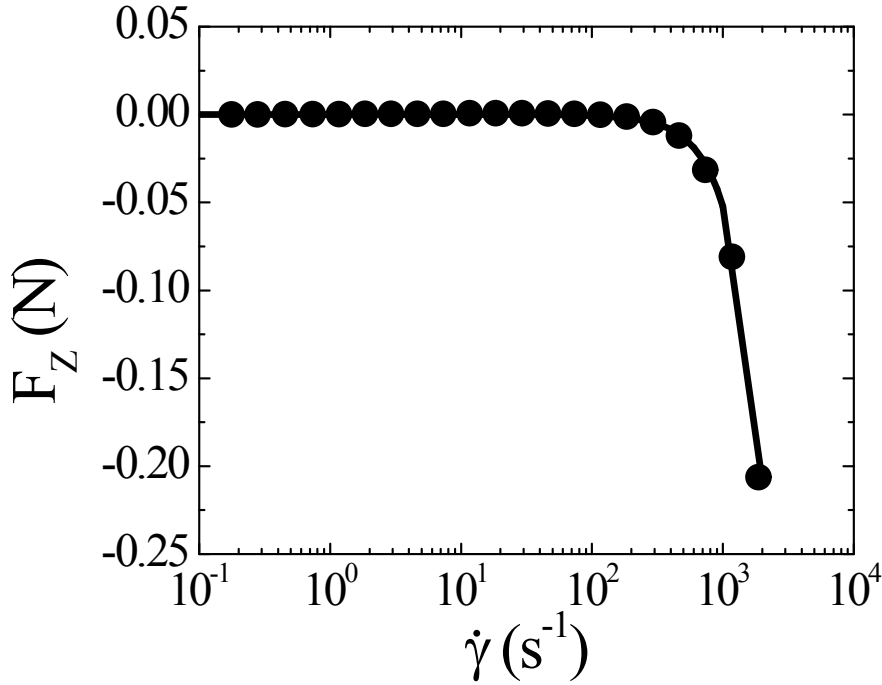


Figure S.1. Measured axial thrust as a function of the applied shear rate for a Newtonian PEG-200 solvent using a 40 mm 2⁰ cone and plate tooling. The solid line is the expected contribution to the axial thrust from inertia given by Equation S.1.

Elastohydrodynamic Scaling at High Stresses

As illustrated in Figure 5, a shear thinning regime follows the shear-thickened state at higher applied shear stresses. Here, a scaling argument for the shear thinning behavior observed at the highest shear stresses probed in this study is proposed. The elastohydrodynamic model originally proposed by Meeker^{85, 86} for single particle deformation near a wall in pastes was extended to colloidal dispersion rheology by Kalman⁸⁷. In this model, the lubrication stresses that give rise to hydrocluster formation are thought to become large enough at high stresses to cause elastic (but not inelastic) deformation of the particle surface. The detailed analysis for the elastohydrodynamic scaling for particles in suspension can be found in Kalman⁸⁷. Ultimately, the limiting value of the viscosity in this shear thinning regime is modelled as:

$$\eta = C \dot{\gamma}^{-1/2} (\eta_f G_o)^{1/2} \quad (\text{S.2})$$

where G_o is the particle modulus and C is a constant that accounts for the on-average proportion of particles in suspension that are in a hydrocluster. The distinguishing feature of this model is the power law scaling of the viscosity with $\dot{\gamma}^{-1/2}$.

In Figure S.2, the steady shear viscosity is plotted as a function of the applied shear rate. The open and closed symbols represent steady flow sweeps performed in opposite directions. This indicates the shear thinning at high shear stresses is reversible and not a consequence of sample ejection, edge fracture, or irreversible particle deformation. The expected elastohydrodynamic power law scaling is shown for the viscosity. The ability of this scaling to capture the behavior of the viscosity at high shear rates suggests elastic deformation of the particles is occurring and is due to the strong lubrication stresses between particle surfaces.

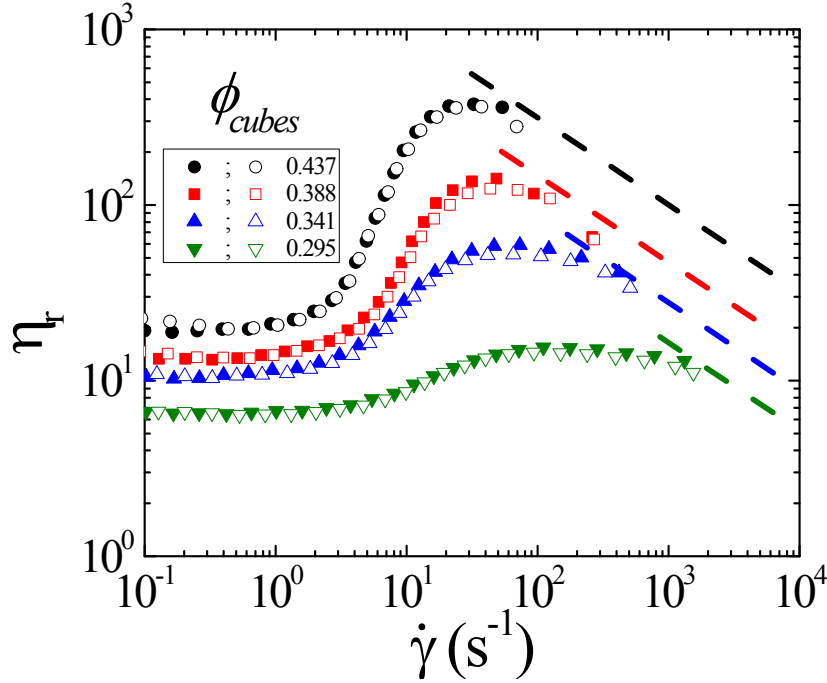


Figure S.2 Predicted elastohydrodynamic scaling (dashed lines) for the relative viscosity as a function of the shear rate for concentrated suspensions of cubic particles.

Steady Shear Creep Experiments

In Figure 6, the time-dependent viscosity of a $\phi_{cubes} = 0.295$ suspension is reported after the imposition of a steady shear creep experiment at $\sigma = 0.1$ Pa starting from an alternance state. This identical experiment was performed on a Newtonian viscosity standard (Cannon) of similar viscosity to the suspension in Figure 6 on the same instrument (AR-2000) and the results are reported in Figure S.3. As shown, there is a lag of approximately 0.66 seconds after the imposition of the steady shear stress (time = 0) before the viscosity reaches its accepted Newtonian value. Thus, the data reported in

Figure 6 is only for times after 0.66 seconds where it can be assured that instrument artifacts are not contributing to the measured viscosity.

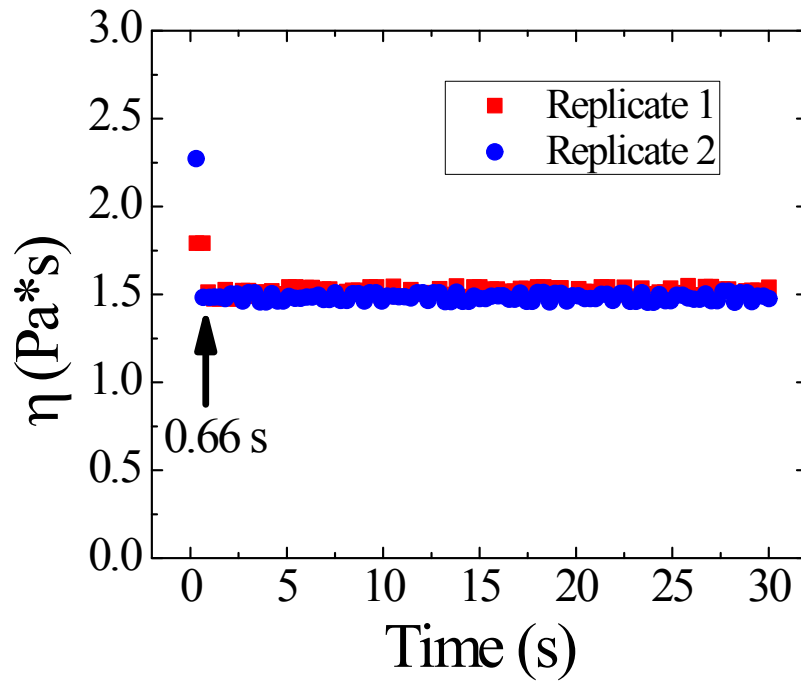


Figure S.3 Steady shear creep experiments performed at $\sigma = 0.1$ Pa on a Newtonian viscosity standard (Cannon) following 300 seconds of oscillation at $\sigma^* = 0.1$ Pa and $\omega = 1$ rad/s. Two replicate experiments were performed to establish the lag time of the instrument.